Methodology for testing a parameter-free fault locator for transmission lines

Popov, Marjan; Parmar, Shreya; Rietveld, Gert; Preston, Gary; Radojevic, Zoran; Terzija, Vladimir

DOI
10.1016/j.epsr.2016.02.007

Publication date
2016

Document Version
Accepted author manuscript

Published in
Electric Power Systems Research

Methodology for testing a parameter-free fault locator for transmission lines

[1]Marjan Popov (Corresponding author), e-mail: M.Popov@tudelft.nl, Tel +31 (0)15 278 6219

[1]Shreya Parmar, e-mail: snuffles91@gmail.com

[2]Gert Rietveld, e-mail: grietveld@vsl.nl

[3]Gary Preston, e-mail: gary.preston@pbworld.com

[4]Zoran Radojevic, e-mail: radojevic@ieee.org

[5]Vladimir Terzija, e-mail: terzija@ieee.org

1. *Delft University of Technology, Faculty of EEMCS, Mekelweg 4, 2628CD, Delft, The Netherlands*
2. *Van Swinden Laboratorium, Delft, The Netherlands*
3. *WSP Parsons Brinckerhoff, Manchester, UK*
4. *Sungkyunkwan University, Suwon, Korea*
5. *The University of Manchester, UK*

Abstract

This paper presents a comparison between two different approaches to fault location both with and without utilising transmission line parameters. Firstly, an impedance-based parameter-dependent algorithm, derived by using modal transformation theory and Fast Fourier Transforms is presented. The methodology is able to locate the fault whether it is on an overhead line or on an underground power cable. The second algorithm is a parameter-free fault location method that uses time synchronized data. Here, the unknown fault location is determined from voltage and current phasors, synchronously measured at both line terminals. This approach to fault location avoids the requirement for prior knowledge of line parameters, which is advantageous as line parameters are not always known precisely. This paper presents the results of algorithm testing through the use of ATPDraw simulations and MATLAB. The results were validated through laboratory experiments. The results of the line parameter-free model are compared with those from the parameter-dependent model. Both algorithms were tested for single line to ground faults.

Keywords: fault location, line parameters, ATPDraw, parameter-free, transmission line,

protection, line impedance.

List of abbreviations

OHL: Overhead Line
EMTP: Electro Magnetic Transients Programme
ATP: Alternate Transients Programme
FLA: Fault Location Algorithm
SMT: Synchronized Measurement Technology
PMU: Phasor Measurement Units
SLG: Single Line to Ground

1. Introduction

Electric power is generated by diverse and dispersed sources, which are often remote from load centres. Transmission lines are essential for transporting the generated power to load centres, and their routes can be very long and through inhospitable terrain. Should a fault occur that cannot be cleared through auto-reclosure, then service crews must be sent to repair the fault; knowledge of where exactly the fault has occurred expedites this process and helps to improve the security and quality of the energy supply [1]. Thus, fault location algorithms have become a very important part of transmission line protection schemes [2], [3], [4].

FLAs are a means accurately determining the distance to a fault on a transmission line from a set reference point, which is usually one of the line terminals.

Whilst there are very many different methods of fault location discussed in the literature, FLAs can be broadly classified into two main types [5]:

- methods based upon travelling wave technology [6], [7], [8];
- methods based upon the transmission line impedance and voltage and current measurements [9], [10], [11], [12].

Impedance-based FLAs measure take voltage and current measurements from one or both ends of the transmission line and utilise suitable circuit analysis techniques to calculate the distance to the fault from the reference point as a function of the transmission line parameters (resistance R, inductance L, and capacitance C per unit length) [13]. However,

these parameters may not be known precisely and they can change with different line loading and weather conditions, which may adversely impact the accuracy of the fault location calculations. In recent years, several papers have been published in which methods of eliminating the negative impact of the line parameters on fault location calculations have been investigated [14], [15], [16], [17], [18], [19]. In each of these cases, the authors developed parameter-free fault location algorithms that were found to deliver accurate calculations of the fault distance when tested with computer simulations.

In this paper, the performance and accuracy of the parameter-free FLAs presented in [14], [15] and [16] are compared with those of a more conventional parameter-dependent FLA. Both fault locators were assessed through computer simulations using EMTP-ATP [20] and MATLAB [21], and the results were validated through laboratory experiments. The results from both algorithms were compared to assess their accuracy.

Section 2 gives detailed derivations of the two FLAs used for this paper; details of the computer simulation testing are given in Section 3; Section 4 presents the results of the laboratory tests; and, finally, the conclusions drawn from this work are given in Section 5.

2. Fault Location Algorithms

A. Parameter-Dependent Algorithm

In this Subsection, the derivation of an impedance-based parameter-dependent FLA is given. Transmission feeders commonly comprise a combination of overhead lines and underground cables; this FLA can locate faults on both. Using Telegraphers' equations, from a single-line representation of a two terminal transmission line model as shown in Fig. 1, voltages and currents on a transmission line can be defined with respect to distance and time. Clarke's transformation is applied to convert the original set of phase variables into a set of 0, α, and β variables. This algorithm uses the work established in [22], [23].

Fig. 1: Schematic representation of a transmission line.

Telegraphers' equations are given as:

$$\frac{\partial v}{\partial x} + L\frac{\partial i}{\partial t} = -Ri \quad (1)$$

$$C\frac{\partial v}{\partial t} + \frac{\partial i}{\partial x} = -Gv \quad (2)$$

where *R*, *L*, *C*, and *G* are the resistance, inductance, capacitance, and conductance of the line/cable per unit length, respectively.

Fig. 2 shows a schematic diagram of three-phase transmission line, with a phase to ground fault at point *F*. *D* is the total length of the transmission line and ℓ is the distance at which fault F occurs from the sending-end terminal (S) of the line. The same F can also be located at a distance (*D*- ℓ) from the receiving end terminal (R) of the line.

Fig. 2: Three-phase representation of a faulted line.

The propagation constant γ and the characteristic impedance of the line Z_C are given as:

$$\gamma = \sqrt{(R + j\omega L)(G + j\omega C)} \quad (3)$$

$$\gamma = \sqrt{(R + j\omega L)(G + j\omega C)}$$

$$Z_c = \sqrt{\frac{R + j\omega L}{G + j\omega C}} \quad (4)$$

$$Z_c = \sqrt{\frac{(R + j\omega L)}{(G + j\omega C)}}$$

Telegraphers' equations (1) and (2) for a single -line can be represented as:

$$\begin{bmatrix} V_x \\ I_x \end{bmatrix} = \begin{bmatrix} \cosh(\gamma x) & Z_c \sinh(\gamma x) \\ \frac{\sinh(\gamma x)}{Z_C} & \cosh(\gamma x) \end{bmatrix} \begin{bmatrix} V_R \\ I_R \end{bmatrix} \quad (5)$$

where V_x, I_x are the voltage and current at any point *x* from the sending end of the line terminal and V_R, I_R are the voltage and current at the receiving-end. Equation (3) can also be

re-written to express V_x, I_x by the sending-end voltages and currents V_S, I_S for a single phase line as:

$$\begin{bmatrix} V_x \\ I_x \end{bmatrix} = \begin{bmatrix} \cosh(\gamma(D-x)) & -Z_c \sinh(\gamma(D-x)) \\ -\frac{\sinh(\gamma(D-x))}{Z_C} & \cosh(\gamma(D-x)) \end{bmatrix} \begin{bmatrix} V_S \\ I_S \end{bmatrix} \quad (6)$$

Where *D* is the total line length and *x* is any point on the line, which can also be represented by the fault point F.

When a fault occurs ℓ km away from the sending end, by making use of above equations, the distance to the fault can be determined by:

$$\ell = \frac{1}{\gamma} tanh^{-1}\left(\frac{A}{B}\right) \quad (7)$$

Here, the constants A and B are given as:

$$A = V_S \cosh(\gamma D) - Z_C I_S \sinh(\gamma D) - V_R \quad (8)$$

$$B = I_R Z_C + V_S \sinh(\gamma D) - Z_C I_S \cosh(\gamma D) \quad (9)$$

By making use of the Clarke's transformation, the single-phase solution can be extended to a three-phase solution:

$$\begin{bmatrix} V_0 \\ V_\alpha \\ V_\beta \end{bmatrix} = T \begin{bmatrix} V_a \\ V_b \\ V_c \end{bmatrix} \quad (10)$$

$$\begin{bmatrix} I_0 \\ I_\alpha \\ I_\beta \end{bmatrix} = T \begin{bmatrix} I_a \\ I_b \\ I_c \end{bmatrix} \quad (11)$$

where $T = \begin{bmatrix} 1 & 1 & 1 \\ 2 & -1 & -1 \\ 0 & \sqrt{3} & -\sqrt{3} \end{bmatrix}$ is Clarkes Transformation.

Hence, the distance to fault in a three-phase system can be shown as:

$$\ell_{0,\alpha,\beta} = \frac{1}{\gamma_i} \tanh^{-1}\left(\frac{A_i}{B_i}\right) \quad (12)$$

Where ℓ_0 is the ground mode, and ℓ_α, ℓ_β are the two areal modes and:

$$\gamma_i = \sqrt{Z_i Y_i} \quad (13)$$

$$Z_{c,i} = \sqrt{Z_i / Y_i} \quad (14)$$

$$Z_{c,i} = \sqrt{Z_i / Y_i}$$

$$A = \boldsymbol{V}_{\mathrm{S},i} \cosh(\gamma_i D) - \boldsymbol{Z}_{c,i} \boldsymbol{I}_{\mathrm{S},i} \sinh(\gamma_i D) - \boldsymbol{V}_{\mathrm{R},i} \quad (15)$$

$$B = \boldsymbol{I}_{\mathrm{R},i} \boldsymbol{Z}_{c,i} + \boldsymbol{V}_{\mathrm{S},i} \sinh(\gamma_i D) - \boldsymbol{Z}_{c,i} \boldsymbol{I}_{\mathrm{S},i} \cosh(\gamma_i D) \quad (16)$$

Accurate fault location can be achieved through selection of the appropriate mode and fault type. The ℓ_α mode is valid for all types of faults except line-line faults, for which the ℓ_β mode is selected.

B. Parameter-Free Algorithm

In this Subsection, the derivation of a parameter-free FLA is given. As discussed in the Introduction, an FLA which does not require prior knowledge of the line parameters algorithm is more flexible and reliable in comparison with more conventional FLAs. The parameter-free algorithm developed in [14], [15], and [16] uses only the fundamental phasors of line voltages and currents sampled at each end of the transmission line. It is not affected by variations in line parameters due to loading or weather conditions, fault impedances, or arc resistances. It can locate all fault types, including balanced three-phase faults, through the use of positive- and negative-sequence current and voltage components. The FFT is applied to extract the fundamental phasors from the voltage and current samples. The FLA was initially derived under the assumption that the data sampling at both ends of the line would be time-synchronised, but was further developed to locate faults without data sampling synchronisation. The data sampling and subsequent phasor extraction is not given special consideration in this paper. It is assumed that both are achieved through the use of advanced SMT and PMUs in [24], [25], [26], [27].

The FLA used here can be used to locate all fault types (single-line-ground, line-line, line-line-ground, and balanced three-phase faults) without recourse to iterative procedures and it

does not need pre-fault data. Furthermore, because it uses only positive and negative-sequence components, it is not affected by zero-sequence coupling.

Using the well-known symmetrical components technique, the positive, negative and zero sequence symmetrical components of the voltages and currents sampled at each end of the line can be determined. The asymmetrical three-phase circuit from Fig. 2 can be represented by three single-phase equivalent circuits: the positive (p), negative (n), and zero (0) sequence circuits. The FLA requires only the positive and negative-sequence components; these are presented in Fig. 3.

a): Equivalent positive sequence circuit of the faulted line.

b): Equivalent negative sequence circuit of the faulted line.

Fig. 3: Symmetrical sequence components of the faulted line.

In the equivalent circuits in Fig. 3, the positive and negative-sequence impedances of the line are equal, so the following equations hold:

$$V_S^p - z\ell I_S^p = V_R^p - z(D-\ell) I_R^p \quad (17)$$

$$V_S^n - z\ell I_S^n = V_R^n - z(D-\ell) I_R^n \quad (18)$$

where $V_S^{p,n}$, $V_R^{p,n}$, $I_S^{p,n}$ and $I_R^{p,n}$ are positive and negative sequence voltages and currents for the sending and receiving ends, respectively; z denotes the positive and negative sequence line impedances, which are equal.

By solving equations (17) and (18), we get:

$$z\ell = \frac{(V_S^p - V_R^p) I_R^n - (V_S^n - V_R^n) I_R^p}{I_S^p I_R^n - I_S^n I_R^p} \quad (19)$$

$$z(D-\ell) = \frac{(V_S^p - V_R^p) I_S^n - (V_S^n - V_R^n) I_S^p}{I_S^p I_R^n - I_S^n I_R^p} \quad (20)$$

The relative distance to the fault, $\ell\%$, can be expressed as a percentage of the line length D as:

$$\ell\% = \frac{z\ell}{z\ell + z(D-\ell)} 100 \quad (21)$$

By rearranging the above equation the solution is obtained:

$$\ell\% = \frac{(V_S^p - V_R^p)I_R^n - (V_S^n - V_R^n)I_R^p}{(V_S^p - V_R^p)(I_S^n + I_R^n) - (V_S^n - V_R^n)(I_S^p + I_R^p)} 100 \quad (22)$$

As it can be seen from the equation, the fault location uses only the symmetrical components of the measured current and voltage phasors from the sending and receiving end of the transmission network. As the fault resistance, R_F, was not used in the development of the proposed algorithm, it does not affect the calculations (this includes arcing faults). It was demonstrated through thorough testing in [14], [15], and [16] that the algorithm is not affected by fault resistance or zero-sequence coupling. Cases of extremely high fault resistance with a corresponding very low fault current are a potential source of inaccuracy due to errors in the current measurements. The algorithm was developed under the assumption that the distances between the phases of the OHL are equal, making the impedance matrix of the OHL symmetrical. The authors of [16] are currently working to assess the effect of unequal phase spacing on the algorithm, and if necessary, develop the FLA further.

The fault location algorithms discussed here can be described by the flow chart given in Fig. 4.

Fig. 4: Flowchart depicting approach used in fault location algorithms.

3. Simulation Results

In this section, the simulation testing of the two FLAs described in the previous section is presented and discussed. The algorithm testing was carried out by simulation analysis using

the internationally recognised ATPDraw software. A 60-km long overhead line with 400kV equivalent infeeds at each end was modelled using ATPDraw, and single-phase to ground faults were simulated along the line. A schematic diagram of the transmission line and equivalent infeeds is shown in Fig. 5.

Fig. 5: Single line diagram depicting the fault line simulations.

The network parameters used for the simulation tests are shown in Table I and the applied line constants are shown in Table II. The impedance and capacitance parameters of the line, which were used for the parameter-dependent fault location algorithm, are listed in Table III.

TABLE I: Network Parameters

TABLE II: Line Parameters

TABLE III: Line Impedance and Capacitance Parameters

Single-line-to-ground (SLG) faults were simulated at different locations along the line through the use of a time-controlled switch. The fault was set to occur at 40 ms. It was assumed that the line was loaded before the fault inception. The sampling frequency was f_S = 25 kHz, and the data window size was 20 ms. This corresponds to N = 500 samples per data window. It was assumed that the sampling synchronisation error was equal to 0 degrees. The phase voltages and currents at both sending- and receiving-end terminals were sampled and used as inputs to both algorithms after relevant variable assignment. The voltage and current waveforms measured at each line terminal are shown in Fig. 6,

a): Receiving end line terminal current waveform.

b): Sending end line terminal current waveform.

c): Receiving end line terminal voltage waveform.

d): Sending end line terminal voltage waveform.

Fig. 6: Sending and receiving-end current and voltage waveforms for a SLG fault at 35 km

along the OHL

Then, the fault location was computed with respect to the sending-end line terminal. Fig. 7 shows the results obtained from both FLAs for an SLG fault at 35 km from the sending-end terminal.

a): Fault location by the parameter-free algorithm.

b): Fault location by the parameter-independent algorithm.

Fig. 7: Estimated fault location from both FLAs for a fault at 35 km from the sending-end.

The results for both algorithms for faults at various distances along the OHL were then compared as shown in the Table IV.

TABLE IV: Simulation Result Comparison

A comparison of the error of the fault distance calculation is shown in the Table V, where the error percentage is given as:

Error = (actual value-calculated value)/(actual value) 100%

TABLE V: Error Percentage Comparison for the FLAs

As can be seen from the results, the error in both FLAs increases as the fault is closer to the ends of the line terminal.

4. Laboratory Testing and Validation

A single-phase high-voltage line test rig was constructed at the VSL Laboratory [26] by connecting six air-cored inductors in series, as shown in Fig. 8.

Fig. 8: Schematics of the experimental setup.

This test rig setup can be used to represent SLG bolted faults on an OHL by directly grounding the test rig at one of the interconnection points between the inductors (points A to E in Fig. 8). The currents and voltages were measured at each relevant point using a

current probe and a voltage divider connected to a high-accuracy digitiser. The measured currents and voltages were then used as inputs to the FLAs.

A. RL Measurements

Measurements were taken to find the *R* and *L* of the air-cored inductors used in the test rig. These measurements were then used to define at which points the test rig should be grounded to replicate SLG faults at different distances along an OHL. The *R* and *L* measurements were taken with the help of an HP3458A multimeter and a precision LCR-meter. The DC resistance measurements were taken using a 4-wire (compensates load resistance) and converter on/off (compensates thermal voltages) measurement method. Care was taken to ensure that the measurements and calibrations were carried out at a fixed temperature.

B. Fault Location on Test Rig

The fault location on the test rig was determined on the basis of the short circuit faults made at points A - E. Assuming a total line length of 60 km, per unit *R*, *L* and impedances for each element were found separately and collectively. Five measurements were performed with the fault made at the five interconnections between the inductors. The fault location in these five measurements was based on the total impedances up to the point representing the sending and the receiving-end. Fault locations on the test rig were calculated by dividing the total line length into segments and finding the respective impedances.

C. Fault Locations as per the Algorithms

A comparison of the results obtained from both FLAs is given in Table VI. Fig. 9 shows the fault distance calculation from both FLAs using measurements taken from the test rig for a representative fault of 19.99 km from the sending-end terminal. The parameter-dependent FLA underestimated the fault distance, whereas the parameter-free FLA overestimated the fault distance.

TABLE VI: COMPARISON OF FLA RESULTS

a): Fault location by the parameter-dependent algorithm.

b): Fault location by the parameter-free algorithm.

Fig. 9: Calculated fault location by the fault location algorithms for a fault simulated at point B on the setup.

5. Conclusions

Faults on transmission lines are a relatively common occurrence. Fault location algorithms are important tools for expediting repairs after the occurrence of a fault on a transmission line.

This paper compares two fault location algorithms developed for use on overhead transmission lines. The first algorithm uses line parameters to locate faults; the second algorithm is independent of the line parameters. Extensive simulations were carried out using ATPDraw simulations and MATLAB to evaluate the performance of both algorithms for single-line to ground faults, which are the most common type of fault on transmission lines. The results from the computer simulations were validated by laboratory testing involving a test rig to replicate single-line to ground faults on an OHL. From the errors observed in the results obtained from both FLAs, the parameter-free FLA gave more accurate calculations of the fault distance compared to the parameter-dependent algorithm.

6. References

[1] Tamronglak, S., Horowitz, SH, Phadke, AG, and Thorp, JS (1996). “Anatomy of power system blackouts: relaying preventive strategies”, Power Delivery, IEEE Transactions on, 11 (2), 708-715.

[2] Kezunovic, M.: "Smart fault location for smart grids" Smart Grid, IEEE Transactions on 2.1 (2011): 11-22.

[3] Saha, M.M., et al. "Review of fault location techniques for distribution systems." Power Systems and Communications Infrastructures for the future, Beijing (2002).

[4] Cook, V. , “Analysis of distance protection”, Vol. 1. Research Studies Press, 1985.

[5] Saha, M. M., et al. “Review of fault location techniques for distribution systems“, Power Systems and Communications Infrastructures for the future, Beijing (2002).

[6] Magnago, F. H. and Abur A.: "Fault location using wavelets" Power Delivery, IEEE Transactions on 13.4 (1998): 1475-1480.

[7] Christopoulos, C., Thomas D.W.P. and Wright A.: "Scheme, based on travelling-waves, for the protection of major transmission lines", IEE Proceedings C (Generation, Transmission and Distribution) Vol. 135. No. 1. IEE, 1988.

[8] Spoor, D. and Zhu J. G.: "Improved single-ended traveling-wave fault-location algorithm based on experience with conventional substation transducers", Power Delivery, IEEE Transactions on 21.3 (2006): 1714-1720.

[9] Hashim, Maher MI, H. Ping W. and Ramachandaramurthy V. K.: "Impedance-based fault location techniques for transmission lines", TENCON 2009-2009 IEEE Region 10 Conference, IEEE, 2009.

[10] Johns, A. T. and Jamali S.: "Accurate fault location technique for power transmission lines." Generation, Transmission and Distribution, IEE Proceedings C. Vol. 137. No. 6. IET, 1990.

[11] Izykowski, J., Rosolowski, E. and Saha M.: "Method and device for fault location in a two-terminal transmission or distribution power line." U.S. Patent No. 8,183,871. 22 May 2012.

[12] Salim, R. H., Salim, K. C. O. and Bretas A. S.: "Further improvements on impedance-based fault location for power distribution systems", IET Generation, Transmission \& Distribution 5.4 (2011): 467-478.

[13] Gopalakrishnan, A., et al.: "Fault location using the distributed parameter transmission line model" Power Delivery, IEEE Transactions on 15.4 (2000): 1169-1174.

[14] Radojević, Z. M., Kim, C., Popov, M., Preston, G., Terzija, V. "New approach for fault location on transmission lines not requiring line parameters" in the Proceeding of IPST Conference, 2009.

[15] Preston, G., Radojević, Z., Terzija, V. 'New Settings-free Fault Location Algorithm Based on Synchronized Sampling'. IET Generation, Transmission and Distribution Journal, Vol. 5, issue 3, pp 376-383, 2011.

[16] Terzija, V., Radojević, Z., Preston, G. 'Flexible Synchronised Measurement Technology-Based Fault Locator'. IEEE Transactions on Smart Grid, Vol. 6, Issue 2, 2015, pp. 866 – 873.

[17] Liao, Y. and Ning K:. "Fault-location algorithms without utilizing line parameters based on the distributed parameter line model", Power Delivery, IEEE Transactions on 24.2 (2009): 579-584.

[18] Apostolopoulos, Christos A., and Korres, G.N.: "A novel algorithm for locating faults on transposed/untransposed transmission lines without utilizing line parameters", Power Delivery, IEEE Transactions on 25.4 (2010): 2328-2338.

[19] Elkalashy, Nagy I. "Simplified parameter-less fault locator using double-end synchronized data for overhead transmission lines", International Transactions on Electrical Energy Systems (2013).

[20] http://www.atpdraw.net

[21] http://nl.mathworks.com/products/matlab/

[22] Popov, M., Rietveld G., Radojević, Z. M, Terzija. V. "An Efficient Algorithm for Fault Location on Mixed Line-Cable Transmission Corridors", in the Proceedings of IPST conference, 2013.

[23] Sayed Tag El Din, El, Abdel Aziz M.M. and Mahmoud G.: "Fault location scheme for combined overhead line with underground power cable", Electric power systems research 76.11 (2006): 928-935.

[24] Xu, Shu-kai, Xiao-rong X. and Yao-zhong X.: "Present application situation and development tendency of synchronous phasor measurement technology based wide area measurement system", Power System Technology 2 (2005): 009.

[25] Phadke, Arun G. and Thorp J., Synchronized phasor measurements and their applications, Springer, 2008.

[26] Novosel, D. and Khoi V.. "Benefits of PMU technology for various applications", Zbornik radova sedmog simpozija o sustavu vođenja EES-a HK CIGRE, Cavtat 5.8.11 (2006).

[27] http://www.smartgrid-metrology.eu/

7.

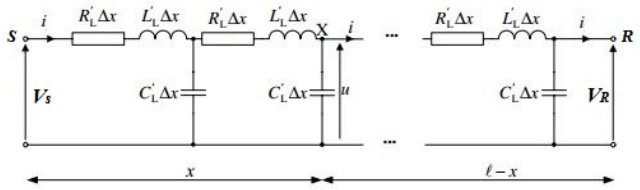

Fig. 1: Schematic representation of a transmission line.

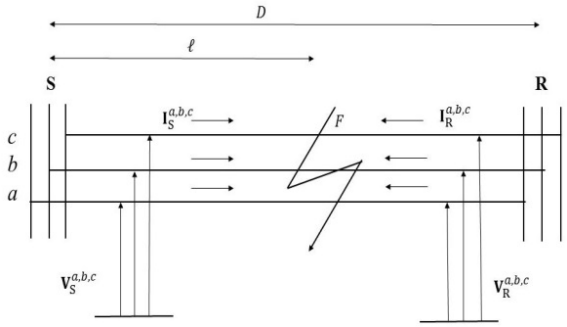

Fig. 2: Three-phase representation of a faulted line.

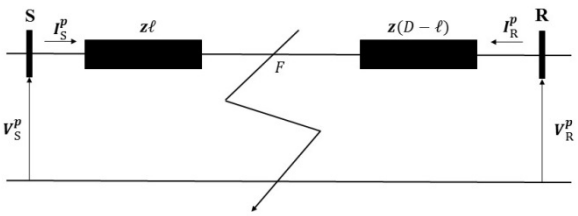

a): Equivalent positive sequence circuit of the faulted line.

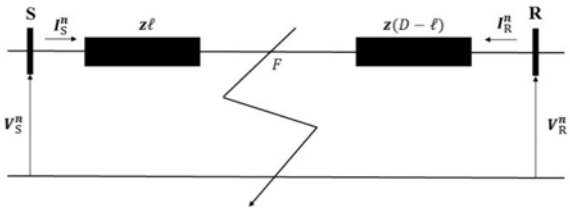

b): Equivalent negative sequence circuit of the faulted line.
Fig. 3: Symmetrical sequence components of the faulted line

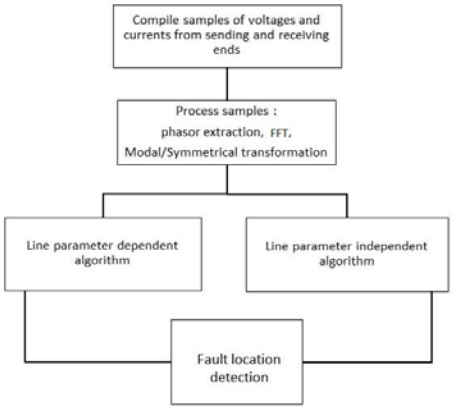

Fig. 4: Flowchart depicting approach used in fault location algorithms

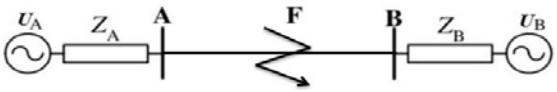

Fig. 5: Single line diagram depicting the fault line simulations

Parameters	Network A	Network B
$U_{LL,rms}$ (KV)	416	400
ϕ (°)	0	-20
R (Ω)	1.0185892	0.6366183
L (H)	0.0509295	0.0318309
R_s(Ω)	2.0371785	1.2732366
L_s(H)	0.1018589	0.0636618

TABLE I: NETWORK PARAMETERS

Parameters	p-n sequence	zero sequence
R (Ω/km)	0.065	0.195
L (mH/km)	0.95493	2.86479

TABLE II: LINE PARAMETERS

Parameters	Values
Z_1 (Ω/km)	0.3317+j0.41634
Z_0 (Ω/km)	0.1972+j0.3699
C_1 (μF/km)	0.008688
C_0 (μF/km)	0.004762

TABLE III: LINE IMPEDANCE AND CAPACITANCE PARAMETERS

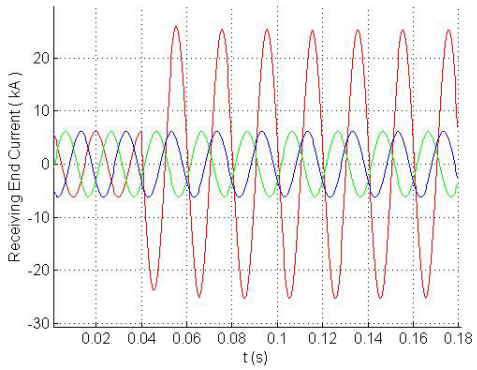

a): Receiving end line terminal current waveform

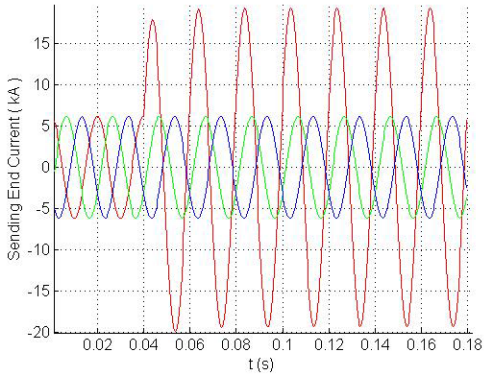

b): Sending end line terminal current waveform.

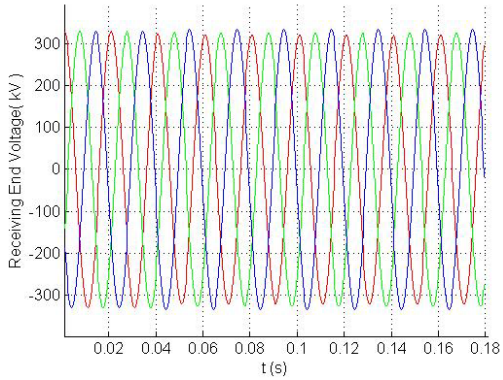

c): Receiving end line terminal voltage waveform

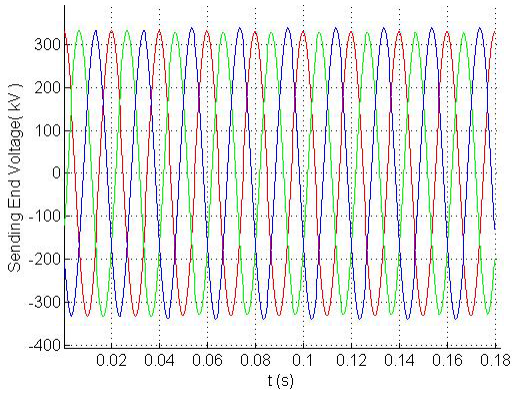

d): Sending end line terminal voltage waveform.

Fig. 6: Sending and receiving-end current and voltage waveforms for a SLG fault at 35 km along the OHL

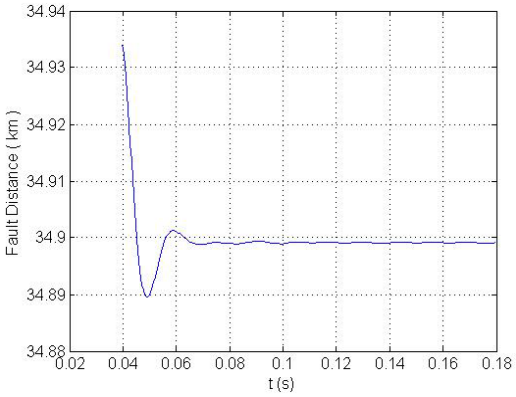

a): Fault location by the parameter-free algorithm.

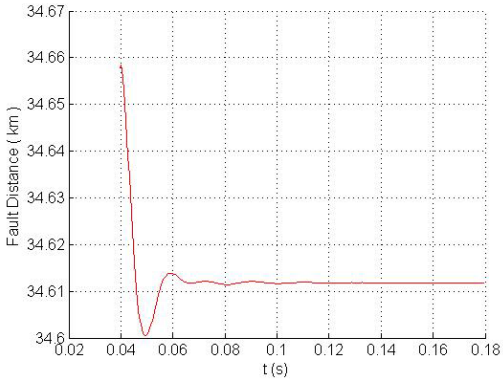

b): Fault location by the parameter-independent algorithm.

Fig. 7: Estimated fault location from both FLAs for a fault at 35 km from the sending-end.

Fault Distance (km)	Parameter-Dependent FLA (km)	Parameter-Free FLA (km)
15	13.897	15.21
20	19.132	20.025
25	24.382	24.873
30	29.638	29.737
35	34.899	34.611
40	40.158	39.487
45	45.426	44.377
50	50.691	49.265
55	55.957	54.154

TABLE IV: SIMULATION RESULT COMPARISON

Actual Fault (km)	Parameter-Dependent FLA error (%)	Parameter-Free FLA error (%)
15	7.353	-1.40
20	4.34	-0.125
25	2.427	0.508
30	1.206	0.875
35	0.288	1.109
40	-0.932	1.384
45	-0.946	1.384
50	-1.382	1.47
55	-1.74	1.538

TABLE V: ERROR PERCENTAGE COMPARISON FOR THE FLAS

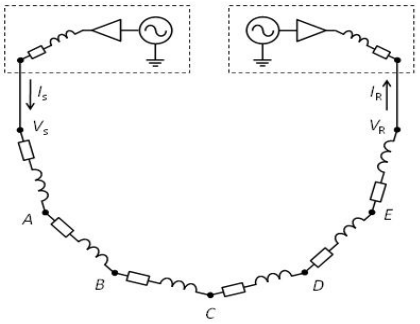

Fig. 8: Schematics of the experimental setup.

Point on Test Rig	Calculated Fault (km)	Parameter-Dependent FLA (km)	Parameter-Free FLA (km)
A	10.04	12.350	10.51
B	19.99	19.354	20.348
C	29.98	27.055	29.732
D	40.02	35.450	39.500
E	50.00	48.850	49.262

TABLE VI: COMPARISON OF FLA RESULTS

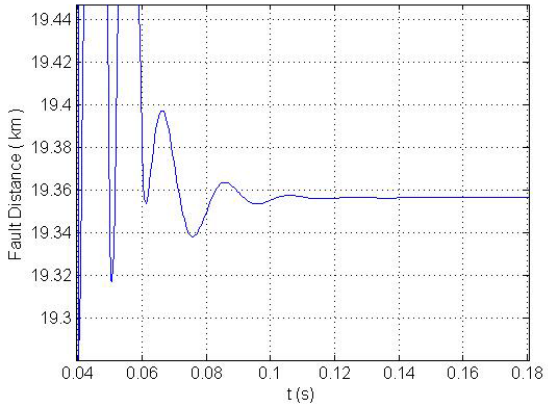

a): Fault location by the parameter-dependent algorithm.

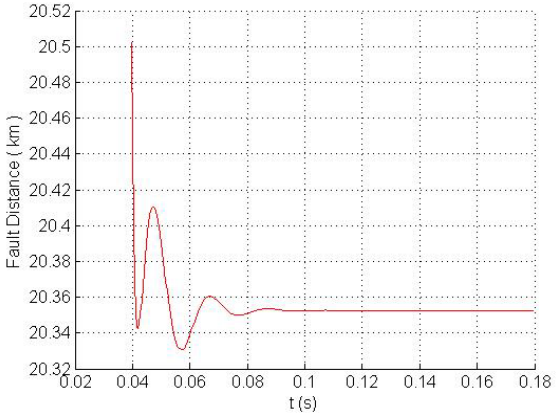

b): Fault location by the parameter-free algorithm.

Fig. 9: Calculated fault location by the fault location algorithms for a fault simulated at point B on the setup.